

CITE AS:

Marchelli F., Cordioli E., Patuzzi F., Sisani E., Barelli L., Baratieri M., Arato E., Bosio B. (2019). Experimental study on H₂S adsorption on gasification char under different operative conditions. *BIOMASS & BIOENERGY*, vol. 126, p. 106-116, ISSN: 0961-9534, doi: 10.1016/j.biombioe.2019.05.003

EXPERIMENTAL STUDY ON H₂S ADSORPTION ON GASIFICATION CHAR UNDER DIFFERENT OPERATIVE CONDITIONS

Filippo Marchelli^{a*}, Eleonora Cordioli^a, Francesco Patuzzi^a, Elena Sisani^b, Linda Barelli^b, Marco Baratieri^a, Elisabetta Arato^c, Barbara Bosio^c

^a Free University of Bozen-Bolzano, Faculty of Science and Technology, Piazza Università 5, 39100 Bolzano (Italy)

^b University of Perugia, Department of Engineering, Via G. Duranti 93, 06125 Perugia (Italy)

^c University of Genova, Department of Civil, Chemical and Environmental Engineering, Via Opera Pia 15, 16145 Genova (Italy)

ABSTRACT: Char, the solid by-product of biomass gasification, usually represents a cost for plant owners, who have to dispose of it at a cost. However, its high carbon content and surface area could make it suitable for further applications, such as adsorption. In this work, we studied its potential for the adsorptive removal of hydrogen sulphide (H₂S), a common pollutant present in the producer gas of gasification, as well as in biogas from anaerobic digestion. Different samples of char collected from commercial gasification plants in South Tyrol (Italy) were tested. The adsorption was reproduced in a lab-scale tubular fixed-bed reactor. The results highlight that all samples could capture hydrogen sulphide, showing different adsorption performances. The surface area of the char and the ash amount seem to affect the removal capacity, although other properties of the materials are probably important. After these tests, we selected the best-performing char, and tested its adsorption performance in different operative conditions, i.e. at different inlet concentrations of H₂S and temperatures.

Keywords: adsorbent, by-product valorisation, fixed bed, gas cleaning, gaseous biofuel, hydrogen sulphide.

1 INTRODUCTION

The gasification of biomass is one of the most promising options to generate energy in a sustainable way. It takes place by putting biomass in contact with a controlled amount of an oxidising agent (oxygen and/or steam), which is less than the amount required for stoichiometric combustion. The whole process occurs at high temperatures (>700 °C). The main product of gasification is a gaseous mixture called producer gas, rich in hydrogen and carbon monoxide. The producer gas can be converted into energy or chemicals through various technologies.

Gasification is a well-established technology, with several commercial plants already built. In the alpine region of South Tyrol (Italy), 46 plants are currently operating, as the map in Fig. 1 shows. Nonetheless, some aspects of the gasification process still need to be optimised [1]. Among these, the production and handling of char greatly affect the economics of the whole process. Char is the solid carbonaceous material produced during gasification and due to the incomplete carbon conversion. Its amount usually ranges between 2% and 5% of the fed biomass [2] and plant owners must dispose of it at a significant cost. In South Tyrol, about 1500 tons of char are produced every year [3], with an associated cost for the disposal of about 150 € ton⁻¹ [4].

[34]. In addition, two different commercial activated carbons, already available in our laboratory at the Free University of Bozen-Bolzano, were employed for comparison purposes. The first activated carbon is Norit GSX. It is obtained from the carbonization of peat at 500 °C, activated with steam at about 1000 °C, and finally washed with hydrochloric acid [35]. This makes it particularly suitable for catalytic applications. The second activated carbon tested for H₂S adsorption is Norit CA1, obtained from wood and chemically activated with phosphoric acid [36]. Norit CA1 is reportedly suitable for the purification of highly colored and foaming liquids for foods and beverages. All the materials are in the form of very fine powders, with particle diameters ranging from 10 to 100 µm.

The properties of all the collected materials are summarised in the following tables. Table 1 indicates the origin of the sampled chars and activated carbons. With respect to the chars, the type of reactor technology from which they were collected is specified, as well as the type of biomass feedstock, and the gasifier operating conditions, in terms of gasifying agent and gasification temperature. For the commercial activated carbons, the precursor feedstock is specified.

Table 2 show the elemental composition of the samples (carbon, hydrogen, nitrogen, sulphur, and oxygen content) and their ash content. Table 3 reports the BET specific surface area (S_{BET}), pore volume size, and pore diameter of each sample.

Table 1 – List of the sampled materials.

Sample	Reactor technology	Feedstock	Gasifying agent	T [°C]
char-A	dual-stage	wood chips	air	900
char-B	downdraft	wood chips	air	800
char-C	rising co-current	wood pellets	air	700
char-D	downdraft	wood chips	air	800
char-E	spouted bed	wood pellets	air	880-900
AC-1	n/a	peat	n/a	n/a
AC-2	n/a	wood	n/a	n/a

Table 2 – Elemental composition of the sampled materials (dry, wt. %).

Sample	C [%]	H [%]	N [%]	S [%]	O [%]	Ash [%]
char-A	78.09	0.37	0.18	0.31	6.43	14.62
char-B	80.64	0.55	0.22	0.20	2.59	15.80
char-C	80.23	0.49	0.23	0.28	2.69	16.08
char-D	48.12	0.49	0.23	0.32	1.32	49.52
char-E	49.90	0.75	0.12	0.32	0.22	48.69
AC-1	90.65	0.39	0.46	0.33	3.71	4.46
AC-2	82.42	1.99	0.19	0.21	12.59	2.60

Table 3 – S_{BET} , pore volume and pore diameter of sampled chars and activated carbons.

Sample	S_{BET} [m ² g ⁻¹]	Pore volume [cm ³ g ⁻¹]	Pore diameter [nm]
char-A	586.72	0.30	3.88
char-B	281.23	0.23	5.22
char-C	127.67	0.28	7.08
char-D	77.90	0.08	8.58
char-E	103.97	0.14	5.18
AC-1	1002	0.51	6.10
AC-2	1269	0.91	5.20

2.2 Bioenergy & Biofuels Laboratory set-up

The first adsorption experiments were performed in the Biofuels and Bioenergy Laboratory of the Free University of Bozen-Bolzano (Italy).

A quartz tubular fixed-bed reactor with length 600 mm and diameter (D) 8 mm was used. In order to keep the sample stable at half height of the reactor, quartz wool was placed above and below the sample. We prepared the gaseous feed with a tank of pure nitrogen and a tank containing a mixture of 1000 ppmv of H₂S in nitrogen, both connected to a mixer that can control and mix the two flows.

The composition of the gas at the exit of the reactor was measured by a micro GC system (Agilent 490 Micro GC).

All tubes and connections were in quartz, PTFE, or stainless steel treated with Sulfinert®. These materials are inert towards hydrogen sulphide, and hence did not adsorb any of it.

The entire setup is schematised in Fig. 2, while the reactor filled with char and quartz wool is depicted in Fig. 3.

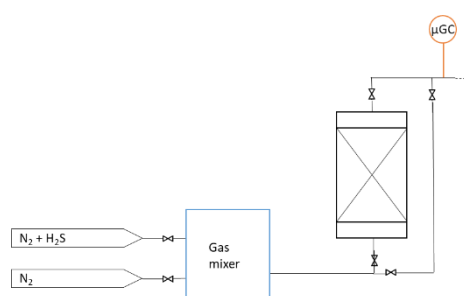


Fig. 2 – Scheme of the adsorption test rig in the Biofuels and Bioenergy Laboratory.



Fig. 3 – Char (above) and quartz wool (below) inside the quartz-tube reactor.

2.3 Fuel Cell Laboratory set-up

Further tests were performed in the Fuel Cell Laboratory of the University of Perugia. This allowed us to confirm the results obtained in Bolzano, as well as to study the effect of higher process temperatures.

In Fuel Cell Laboratory, dynamic adsorption runs on char-A samples were performed using the test bench shown in Fig. 4. The sorbent was placed in a fixed-bed flow reactor made of quartz (inner diameter 18 mm, length 200 mm) and located on a quartz porous sieve (100-160 μm, G1 porosity). The reactor temperature was controlled by TR1 and TC1 devices (producer: Watlow), using an external spiral heater (RH, producer: Watlow), while the temperature of the reaction chamber was measured with a thermocouple (TC3). Quartz was chosen as material for the reactor for its resistance to high temperatures and for its inertness towards hydrogen sulphide.

The inlet gas mixtures were prepared using 1000 ppmv of H₂S in N₂ matrix, diluted with pure nitrogen by means of gas mass flow meter controllers (GFCs, producer: Bronkhorst High-Tech). H₂S level at reactor outlet was monitored using an electrochemical gas sensor (ES, producer: Recom Ind. srl), executing an immediate concentration reading in the range 0 - 25 ppmv (accuracy 0.1 ppmv), with acquisition time steps of 10 s.

Pipelines and fittings are made of PTFE or stainless steel treated with Sulfinert®, to avoid H₂S

adsorption on working surfaces, preserving the introduced amount of active sulphur species. Cable heaters (CH) are employed to pre-heat the inlet gas mixture, maintaining the pipelines at the same temperature of the reactor. Air is used after each run to remove possible adsorbed sulphur molecules inside the system and to guarantee the correct operation of the detection system.

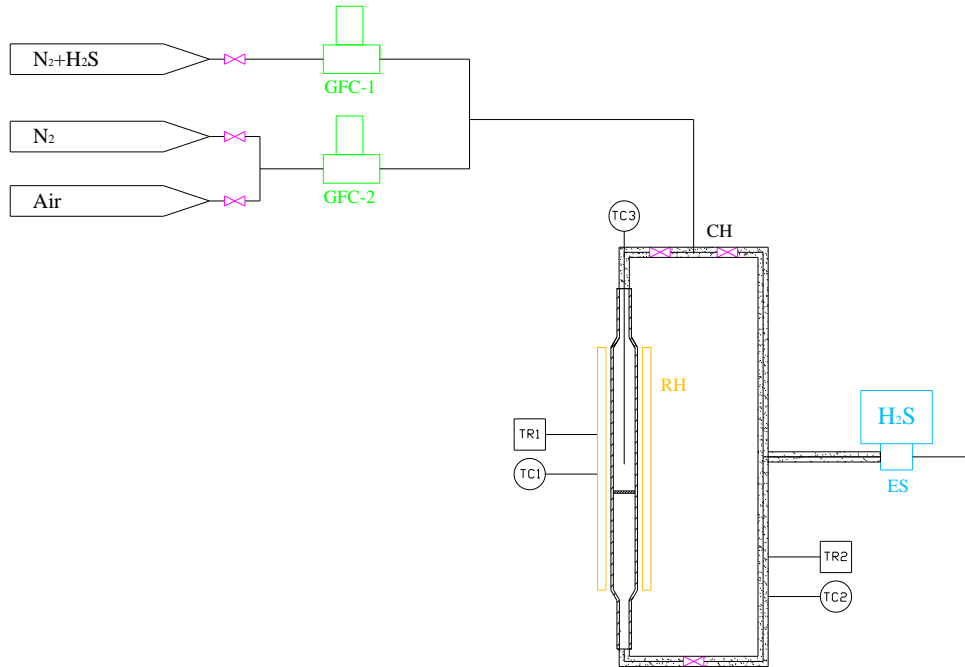


Fig. 4 – Scheme of the adsorption test rig in the Fuel Cell Laboratory.

2.4 Experimental procedure

Prior to testing adsorption capacity of the samples, char and activated carbons were degassed and dried at 105 °C overnight. Inside the reactor, we put a certain amount of material, so that the height of the filter was 2.5 cm, which resulted in acceptable pressure drops (see Section 3.5). The corresponding ratio between the filter height (h) and diameter (D) was 3.13. In the subsequent tests, performed in Perugia, the h/D ratio was kept constant.

In the first set of experiments, the total flow of the gas was set to 100 Nml min⁻¹, which corresponds to a velocity of 3.33 cm s⁻¹ in empty column. This is inferior to the typical values of gas flow found in industrial-scale processes, in which the velocity ranges between 14 and 17 cm s⁻¹ [32]. This choice was done in order to avoid the formation of excessive pressure drops in the reactor, too. In fact, given that both chars and activated carbons were composed of extremely fine particles, setting an excessively high gas flow would cause a high pressure zone above the packed bed and would make it slip through the reactor, invalidating the test.

In the tests performed in Perugia, the inlet gas flow rate was set to 1140 Nml min⁻¹ in order to keep constant the value of the gas hourly space velocity (GHSV).

Table 4 summarises the operative conditions chosen for the experiments. An inlet concentration of H₂S equal to 250 ppmv was selected to study the adsorption capacity of the samples. This concentration was then changed (increased up to 1000 ppmv) in order to investigate any effect of the inlet concentration on the adsorption capacity.

Table 4 – Operative conditions of the experiments (*=experiments performed in Bolzano, **=experiments performed in Perugia)

Variable	Value
Height of the fixed bed	2.5 cm
h/D	3.13

Sample mass	<ul style="list-style-type: none"> • 150 to 200 mg * • 1.86 g **
Total gas flow rate	<ul style="list-style-type: none"> • 100 Nml min⁻¹ * • 1140 Nml min⁻¹ **
GHSV	4775 h ⁻¹
Inlet concentration of H₂S (in N₂)	<ul style="list-style-type: none"> • 250 ppmv to study the adsorption capacity • 250 to 1000 ppmv to study the influence of the H₂S inlet concentration
Temperature	<ul style="list-style-type: none"> • Ambient * • 298, 323, 363 K **
Pressure	Atmospheric

At the beginning of each test, we let pure nitrogen (N₂) flow into the reactor in order to let all the oxygen out, and then we started feeding the H₂S/N₂ mixture. The composition of the outflow gas was continuously monitored. We performed each experiment at least twice. In the experiments performed in Bolzano, the concentration of H₂S at the outlet of the reactor could be sampled for any concentration, but the measurement could only be performed every three minutes. Conversely, the analyser in Perugia could measure the outlet H₂S concentration every ten seconds, but only for values up to 25 ppmv. For this reason, the tests performed in Bolzano were stopped when the outlet concentration of H₂S was equal to 95% of the inlet concentration. The tests in Perugia were instead stopped when the outlet concentration of H₂S was equal to 1 ppmv. Despite this difference, the analyses are fully comparable, because for the tests performed in the same conditions, the amount of H₂S adsorbed in the first stage of the process is the same.

After the analyses in Bolzano, we measured the final elemental composition of the char or AC sample with a Vario MACRO Cube Elementar Analyzer, in order to detect any increase in the sulphur content.

For both experimental sets, thanks to the continuous monitoring of the outlet flow concentration, it was possible to calculate the quantity of H₂S that each sample adsorbed in the experiments. We numerically calculated the following integral, based on the mass balance of the reactor and on the ideal gas law:

$$m_{ads} = \frac{M \cdot P \cdot Q}{R \cdot T \cdot m_{char}} \int_0^{t_{fin}} (c_{in} - c_{out}) dt$$

in which:

- m_{ads} is the adsorbed amount of H₂S per gram of adsorbent [mg g⁻¹];
- M is the molar mass of H₂S (34.0818 g mol⁻¹);
- P is the pressure (1.0315 · 10⁵ Pa)
- Q is the total gas flow rate, hypothesised to be constant throughout each analysis since the variation due to the H₂S adsorption is negligible [ml min⁻¹];
- R is the gas constant (8.314 J · mol⁻¹ · K⁻¹);
- T is the absolute temperature [K];
- m_{char} is the mass of char employed in the test [g];
- t_{fin} is the duration of the experiment [min];
- c_{in} and c_{out} are the concentrations of H₂S at the inlet and outlet of the reactor, respectively [-].

As already stated, the adsorption capacity calculated for the experiments in Bolzano is referred to saturation conditions. Conversely, the adsorption capacity calculated for the experiments in Perugia is referred to the amount that the material could capture before the H₂S concentration at the outlet was 1 ppmv.

After the experiments performed in Perugia, the desorption process was also studied. With an analogous procedure, the reactor containing the used sample was fed with an N₂ flow of 1667 Nml min⁻¹ at 100°C.

3 RESULTS AND DISCUSSION

3.1 Adsorption capacity of the tested materials

The first set of experiments allowed us to calculate the maximum H₂S adsorption capacity of each sample. Table 5 reports the results of the tests.

Table 5 – H₂S adsorption capacities of the studied chars and activated carbons.

Sample	Adsorption capacity [mg g ⁻¹]
char-A	6.88 ± 0.37
char-B	5.41 ± 0.26
char-C	5.38 ± 0.57
char-D	2.77 ± 0.08
char-E	1.61 ± 0.02
AC-1	2.35
AC-2	2.61 ± 0.05

The results confirm that the studied chars and activated carbons were able to capture H₂S with different efficiency depending on their specific properties.

The activated carbons (samples AC-1 and AC-2) performed poorly and adsorbed less H₂S than most of the chars. This might be caused by the type of activation process, which makes these activated carbons particularly suitable for applications different from gas adsorption, as their specifications report. In fact, this is not in contrast with results obtained in a previous study [23], in which a certain type of activated carbon adsorbed only 1.71 mg_{H₂S} g⁻¹ before the breakthrough, very little compared to other types that were able to remove up to 27.15 mg_{H₂S} g⁻¹. In that case, the reason was identified in the fact that the best performing activated carbons were impregnated with copper and chromium salts or potassium hydroxide. This indicated that the removal was not only promoted by micropores, but also by chemical reactions such as sulphide salts formation or acid-base neutralization.

As regards the experiments performed in the present study, we did not pre-treat the chars with chemicals nor activated them physically. However, all the chars feature a high percentage of ash, and we speculate that they might contain compounds that enhance their H₂S adsorption capacity. Indeed, our research group already detected the presence of heavy metals in gasification char in a previous study [37].

Fig. 5 shows a plot in which the specific adsorption capacity of each sample is related to its surface area. For the chars, higher values of surface area seem to affect adsorption positively. However, the trend is not always increasing and it is likely that the adsorption capacity also depends on other factors. The two activated carbons feature a much higher specific surface area, but their adsorption capacity is lower than the best performing chars.

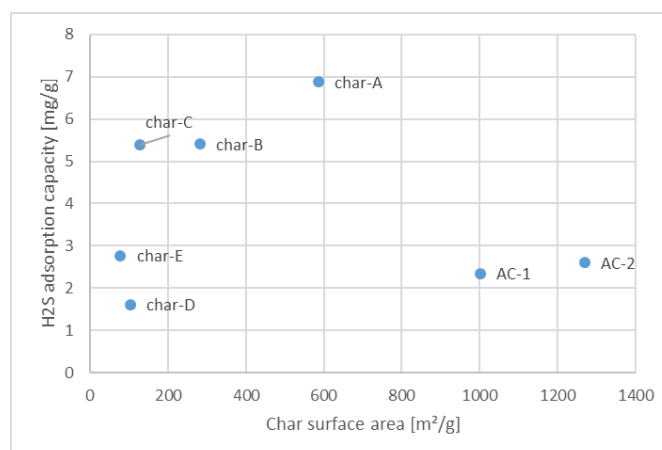


Fig. 5 – Dependency of the adsorption capacity of char and activated carbon samples on the BET surface area.

Looking at the graph, the fact char-C adsorbs about twice the amount of chars D and E and about the same as chars A and B is hardly understandable by a simple comparison of the material properties that have been studied. The same can be said about the better performance of char-D compared to char-E, despite its lower surface area. Clearly, more in-depth analyses are required to identify the most relevant properties affecting the adsorption capacity.

The specific adsorption capacity can also be related to the ash content, as shown in Fig. 6. Even in this case, there is no overall trend, but it seems that a very high or very low amount of ash corresponds to a decrease in the adsorption capacity. Nonetheless, it is likely that the composition of the ash has a role, in addition to the amount.

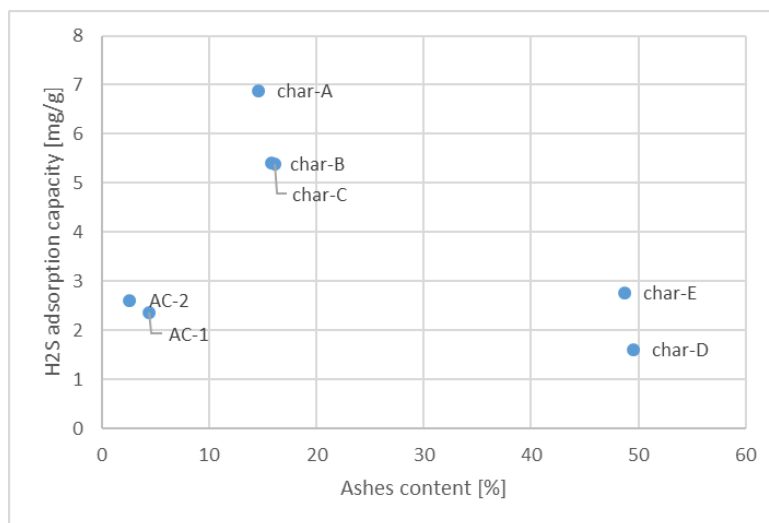


Fig. 6 – Dependency of the char adsorption capacity on the ash content.

The values of adsorption capacity are anyway interesting and promising for a real scale application of these materials. To confirm this, it is possible to compare them with literature data, some of which are summarised in Table 6.

Table 6 – Adsorption capacities of some materials from literature.

Material	Adsorption capacity [mg g ⁻¹]	Reference
AC RGM1	>27.15	[23]
AC RBAA1	>20.43	[23]
Alumina Galipur	>1.56	[23]
AC RB1	>1.71	[23]
Zeolite ATZ	<0.1	[23]
Sepiolite	<0.1	[23]
KOH/CaO impregnated activated carbon	>130	[30]
Char from pyrolysis of used wood pellets	0.04	[32]
- same after activation	12.92	[32]
Char from pyrolysis of food waste and coagulation-flocculation sludge	0.22	[32]
- same after activation	66.60	[32]
AC Desotec Airpel Ultra DS	>34.87	[38]
Carbon fibers	800	[28]
Potassium hydroxide AC	65	[39]
Copper impregnated AC	46.3	[40]

The reported activated carbons were either commercial or specifically synthesised by the authors. Most of these activated carbons can adsorb more H₂S than the chars studied in the present work. However, in the current moment, gasification char represents a waste, so not only it has no purchasing cost, but it represents a cost for the plant owners that have to dispose of it. Moreover, several of the materials in Table 6 underwent activation phases, in some cases even with chemical compounds, which increased their efficiency. On the other hand, the chars we studied were able to adsorb H₂S in the form at which they left the plant, only after a degassing phase, and their capacity was higher than the one reported for untreated pyrolysis chars [32]. Pyrolytic chars reportedly perform better only after activation with steam at 850 °C. The fact that the chars collected from local gasification plants showed good performances without any further processing makes them good and cheap candidates for H₂S adsorption applications.

3.2 Influence of the H₂S inlet concentration

Char-A was the sample with the highest adsorption capacity; hence we chose it for further experiments.

In particular, we performed tests with different inlet concentrations of H₂S, in order to assess the influence on the adsorption process. Three values of H₂S inlet concentration were chosen: 250, 500, and 1000 ppmv.

Fig. 7 depicts three representative breakthrough curves for the three studied inlet concentrations. As expected, a higher concentration saturates the adsorbent faster, so the outlet concentration becomes equal to the inlet one in a shorter time.

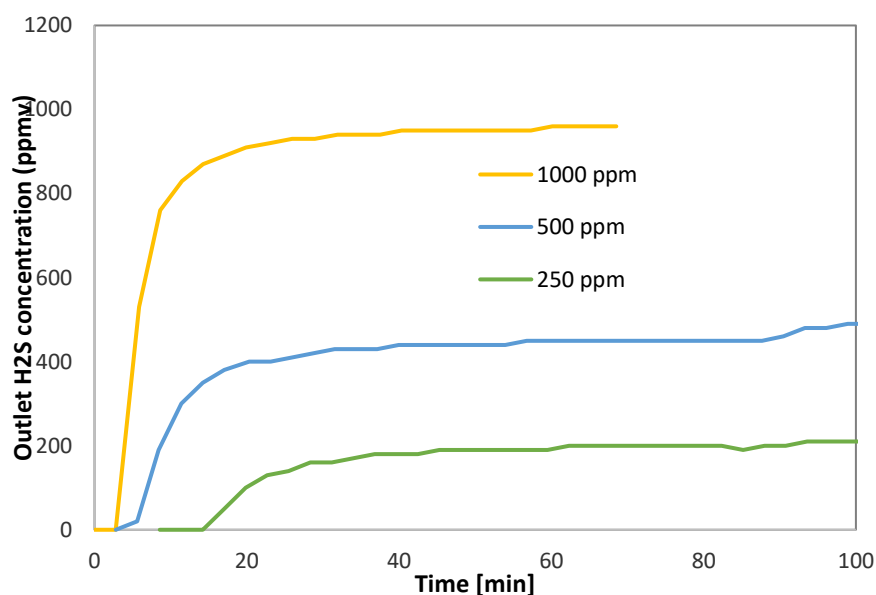


Fig. 7 – Breakthrough curves for different inlet concentrations of H₂S

Table 7 reports the saturation adsorption capacities for the three inlet concentrations. It does not show a clear trend. It can be concluded that, in the studied interval, the inlet concentration of H₂S does not significantly affect the maximum adsorption capacity.

Table 7 – Maximum adsorption capacity for different inlet concentrations of H₂S

Inlet concentration of H ₂ S [ppmv]	Maximum H ₂ S adsorption capacity [mg g ⁻¹]
250	6.88 ± 0.37
500	7.87 ± 0.70
1000	6.98 ± 0.24

3.3 Influence of the process temperature

Char-A was also used to test the influence of temperature on the adsorption performance. Three values were studied: 298, 323, and 363 K.

Fig. 8 shows the breakthrough curves for the three cases. As it can be observed, the higher the process temperature, the better the adsorption performance is. At ambient temperature, the filter manages to capture all of the fed H₂S for approximately 7.667 minutes, after which H₂S starts being detected at the outlet. This time value increases to 9.833 and 13.167 minutes for the cases at 323 and 363 K, respectively. This is counterintuitive, since adsorption is hindered by an increase in temperature. The effect can be ascribed to the increase in pressure caused by the increase in temperature, which also creates a higher partial pressure of H₂S inside the bed. The formation of a high pressure gradient is confirmed by the fact that, for higher temperatures (such as 398 K), the reactor unsealed the experiment had to be stopped. In the future, we will try to perform experiments with a significantly lower h/D ratio, in order to assess whether this can allow avoiding the pressure effect..

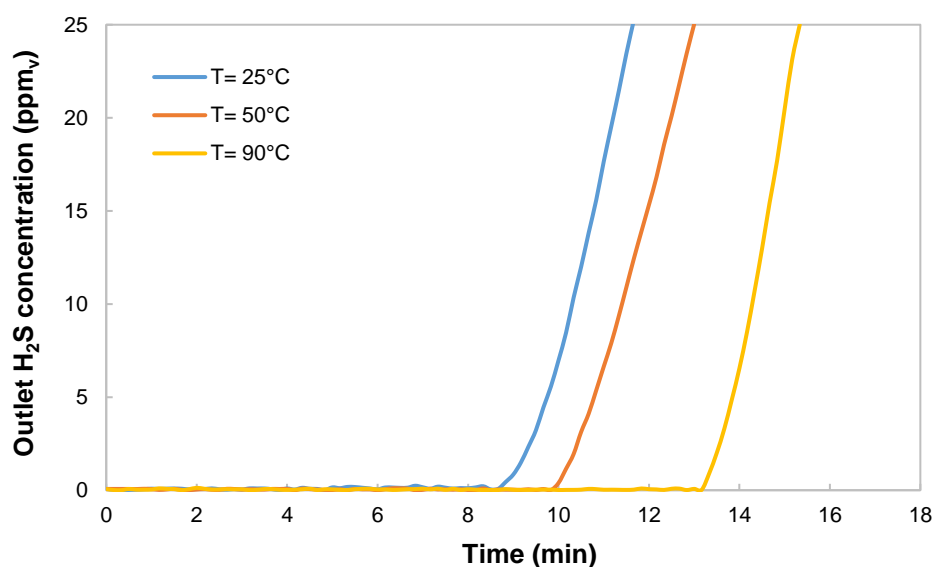


Fig. 8 – Breakthrough curves obtained at different temperatures.

Table 8 displays the amount of H₂S captured by char-A at the three different temperatures. The time value t_0 represents the last instant for which a concentration of 0 ppmv is detected, while t_1 represents the first instant for which a concentration of 1 ppmv is detected. At higher temperatures, the char can adsorb all of the H₂S for a longer time, and this is reflected in the adsorption capacities. With a 65 K increase, the adsorption capacity is enhanced by 46%.

Table 8 – Breakthrough times and adsorption capacity of char-A at different temperatures.

Temperature (K)	t_0 (min)	t_1 (min)	$C_{1 \text{ ppmv}}$ (mg/g)
298	7.667	9.167	2.13 ± 0.03
323	9.833	10.167	2.36 ± 0.03
363	13.167	13.333	3.10 ± 0.04

3.4 CHNS results

After the adsorption experiments, the used chars and activated carbons were subjected to CHNS analyses again, in order to detect any changes in their elemental composition. Table 9 shows the results of the analyses. Unfortunately, the quartz wool used in the experiments heavily polluted the samples, so the results were inaccurate and performing a mass balance was not possible. Despite this, the results permitted to draw some qualitative conclusions that will be discussed in the following.

Table 9 – Results of the CHNS analyses on the used samples after H₂S adsorption (wt. %).

Sample	C [%]	H [%]	N [%]	S [%]
char-A (250 ppmv)	44.63	0.05	0.09	0.53
char-A (500 ppmv)	52.05	0.16	0.12	0.48
char-A (1000 ppmv)	60.12	0.19	0.15	0.51
char-B	76.95	0.48	0.28	0.58
char-C	81.10	0.59	0.31	0.63
char-D	42.43	0.29	0.22	0.82
char-E	52.14	0.49	0.29	0.38
AC-1	85.47	0.30	0.41	0.84
AC-2	70.21	2.40	0.15	0.28

Fig. 9 reports the variation in carbon and sulphur content for each sample. It can be seen that the carbon content differs from the original value, mostly with a decreasing trend, which is probably caused by the quartz wool. On the contrary, the sulphur content presents an opposite trend and increases in all cases. This can confirm that sulphur is adsorbed onto the char and activated carbon surfaces.

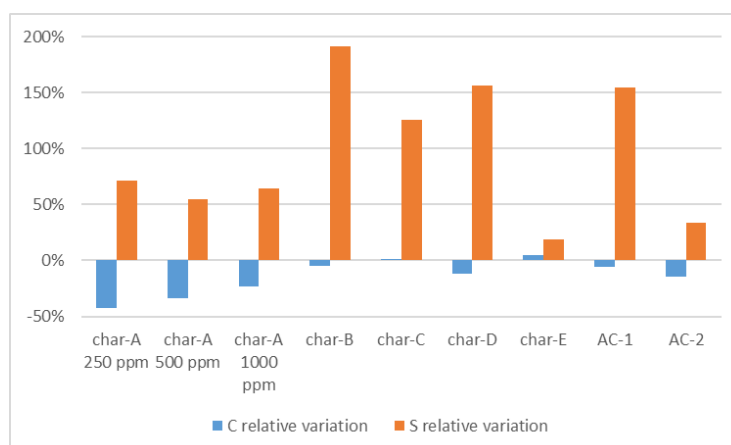


Fig. 9 – Relative variation of C and S after the adsorption experiments.

3.5 Pressure drops

The chars that were collected from commercial gasification plants are very fine materials. A zeta-analysis on char-A, for instance, reported an average diameter of about 50 μm . With a density of 480 g l^{-1} , this char belongs to the Group C (or “cohesive”) of the Geldart classification, which classifies powders according to their fluidization properties [41]. The materials belonging to this group have very strong interparticle forces, which greatly affect the fluidization behaviour of the powder. In small diameter tubes, like the one used for the experiments presented in this work, as the gas flow through the bed is increased, the powder slips as a plug in the reactor or channels severely.

With the aid of a manometer, we analysed the pressure drops that arose in the reactor containing a bed of char-A. Pure nitrogen (N_2) was fluxed through the tubular reactor for performing the pressure drop tests.

When the mass of char was 100 mg and the bed height about 1.25 cm, the pressure drop was lower than 10 kPa for a flow up to 650 Nml min^{-1} . By increasing the flow to 950 Nml min^{-1} , the pressure drop increased to 30 kPa.

By doubling the amount of sample in the char bed, the pressure drop was observed to be lower than 10 kPa for a flow up to 350 Nml min^{-1} . Then, it increased to 32 kPa for a flow of 550 Nml min^{-1} . A further increase in the flow made the char bed unstable and nullified the tests.

These observations suggest that the very fine nature of the studied chars might hinder their application in real-scale setups. Very high pressure drops could arise, and channelling or dragging phenomena may take place. Increasing the size of these materials, for instance by pelletising them, could enhance the feasibility of their use. However, some deep investigation should be done case by case, since pressure drops through the reactor depend on its size and geometry, and on the specific operating conditions [42].

4 CONCLUSIONS

In this work, we studied the adsorption of hydrogen sulphide (H_2S) on residual char from biomass gasification and on activated carbon. We employed five different samples of biomass char (collected from either commercial or pilot plants), and two commercial activated carbons available in our laboratory.

All the studied chars were able to adsorb H_2S , with better performances than the two activated carbons. The maximum adsorption capacity that was reached is 6.88 mg of H_2S per gram of char. However, a comparison with literature data showed that the adsorption capacity obtained is lower than that of the best performing activated carbons, which are, usually, chemically activated. On the other hand, the adsorption capacity of the studied gasification chars is higher than that of untreated pyrolysis chars.

The total adsorption capacity seems to be related to the specific surface area of the char, although the relation is not linear and other factors most likely affect the phenomenon. The ash content seems to influence the adsorption capacity as well. In particular, very high or very low percentages of ash seem to hinder the H_2S adsorption. However, it is likely that not only the amount of ash, but also its composition might be relevant to the efficacy of the adsorption process.

Within the studied range, from 250 to 1000 ppmv, the inlet concentration of H_2S affects the speed of the process, as predictable. Hence, the higher the concentration of hydrogen sulphide fed, the shorter is the time needed for the adsorbent to reach saturation. On the other hand, it was observed that the inlet concentration does not affect the saturation.

The process temperature also affects the adsorption performance. In particular, higher temperatures have a positive impact on the amount of H_2S adsorbed by the char. It is speculated that this effect is actually caused by a pressure increase inside the reactor, originated by the temperature increase. Future experiments performed with a lower h/D ratio will investigate this effect.

The adsorption of H_2S on the surface and in the pores of the samples was also confirmed through CHNS analyses, which highlighted an increase in the sulphur content even though the samples were heavily polluted by quartz wool.

Further studies might help to understand the phenomenon. In fact, it is clear that specific surface area, microporosity, and ash composition influence the H_2S adsorption activity, but it is still not fully understood which property of the char majorly affects it. Moreover, other operative conditions could be studied, including the adsorption of H_2S in a test or real producer gas (or biogas) instead of using pure nitrogen. Furthermore, the performance of char could be enhanced through either thermal or chemical activation, and its particle size might be increased to avoid great pressure drops in the reactor and hence enhance the usability of this by-product.

Nonetheless, these preliminary results are very promising and confirm that gasification char could be very useful for improving significantly the overall efficiency of gasification plants, from an energetic, but also economic point of view. Plant owners could avoid the costs for its disposal and those for the purchase of a commercially available H_2S adsorbent, thus following the principles of the circular economy and reducing the environmental impact of the whole gasification process.

5 ACKNOWLEDGMENTS

This work was supported by the Autonomous Province of Bolzano, Provincia Autonoma di Bolzano – Alto Adige, Ripartizione Diritto allo studio, Università e ricerca scientifica, through the NEXT GENERATION project: “Novel EXTension of biomass poly-GENERATION to small scale gasification systems in South-Tyrol” (CUP B56J16000780003).

6 REFERENCES

- [1] A. Molino, S. Chianese, D. Musmarra, Biomass gasification technology: The state of the art overview, *J. Energy Chem.* 25 (2016) 10–25. doi:10.1016/j.jechem.2015.11.005.
- [2] S. Vakalis, A. Sotiropoulos, K. Moustakas, D. Malamis, M. Baratieri, Utilisation of biomass gasification by-products for onsite energy production, *Waste Manag. Res.* 34 (2016) 564–571. doi:10.1177/0734242X16643178.
- [3] E. Cordioli, F. Patuzzi, M. Baratieri, Experimental and Modelling Analysis of Char Decomposition: Experiences with Real Scale Gasification Systems, *Energy Procedia.* 105 (2017) 724–729. doi:10.1016/j.egypro.2017.03.382.
- [4] D. Basso, F. Patuzzi, A. Gasparella, W. Tirler, S. Dal Savio, A.M. Rizzo, D. Chiaramonti, M. Baratieri, Valorization Pathways for Char from Small Scale Gasification Systems in South-Tyrol: The Next Generation Project, *Eur. Biomass Conf. Exhib. Proc.* (2017) 747–750. doi:10.5071/25theubce2017-2cv.3.10.
- [5] V. Benedetti, F. Patuzzi, M. Baratieri, Characterization of char from biomass gasification and its similarities with activated carbon in adsorption applications, *Appl. Energy.* (2017) 1–8. doi:10.1016/j.apenergy.2017.08.076.
- [6] D. Dias, N. Lapa, M. Bernardo, D. Godinho, I. Fonseca, M. Miranda, F. Pinto, F. Lemos, Properties of chars from the gasification and pyrolysis of rice waste streams towards their valorisation as adsorbent materials, *Waste Manag.* 65 (2017) 186–194. doi:10.1016/J.WASMAN.2017.04.011.
- [7] J.J. Hernández, M. Lapuerta, E. Monedero, Characterisation of residual char from biomass gasification: effect of the gasifier operating conditions, *J. Clean. Prod.* 138 (2016) 83–93. doi:10.1016/j.jclepro.2016.05.120.
- [8] M. Barbanera, F. Cotana, U. Di Matteo, Co-combustion performance and kinetic study of solid digestate with gasification biochar, *Renew. Energy.* 121 (2018) 597–605. doi:10.1016/J.RENENE.2018.01.076.
- [9] M. Inyang, E. Dickenson, The potential role of biochar in the removal of organic and microbial contaminants from potable and reuse water: A review, *Chemosphere.* 134 (2015) 232–240. doi:10.1016/j.chemosphere.2015.03.072.
- [10] M. Ahmad, A.U. Rajapaksha, J.E. Lim, M. Zhang, N. Bolan, D. Mohan, M. Vithanage, S.S. Lee, Y.S. Ok, Biochar as a sorbent for contaminant management in soil and water: A review, *Chemosphere.* 99 (2014) 19–33. doi:10.1016/j.chemosphere.2013.10.071.
- [11] D. Mohan, A. Sarswat, Y.S. Ok, C.U. Pittman, Organic and inorganic contaminants removal from water with biochar, a renewable, low cost and sustainable adsorbent – A critical review, *Bioresour. Technol.* 160 (2014) 191–202. doi:10.1016/j.biortech.2014.01.120.
- [12] A.E. Creamer, B. Gao, Carbon-Based Adsorbents for Postcombustion CO₂ Capture: A Critical Review, *Environ. Sci. Technol.* 50 (2016) 7276–7289. doi:10.1021/acs.est.6b00627.
- [13] E. David, J. Kopac, Activated carbons derived from residual biomass pyrolysis and their CO₂ adsorption capacity, *J. Anal. Appl. Pyrolysis.* 110 (2014) 322–332. doi:10.1016/j.jaap.2014.09.021.
- [14] A.S. González, M.G. Plaza, F. Rubiera, C. Pevida, Sustainable biomass-based carbon adsorbents for post-combustion CO₂ capture, *Chem. Eng. J.* 230 (2013) 456–465. doi:10.1016/j.cej.2013.06.118.
- [15] G. Ravenni, Z. Sárossy, J. Ahrenfeldt, U.B. Henriksen, Activity of chars and activated carbons for removal and decomposition of tar model compounds – A review, *Renew. Sustain. Energy Rev.* 94 (2018) 1044–1056. doi:10.1016/J.RSER.2018.07.001.
- [16] S. Pedrazzi, G. Allesina, L. Sebastianelli, M. Puglia, N. Morselli, P. Tartarini, Chemically Enhanced Char for Syngas Filtering Purposes, *Eur. Biomass Conf. Exhib. Proc.* (2018) 694–698. doi:10.5071/26theubce2018-2cv.2.7.
- [17] P.J. Woolcock, R.C. Brown, A review of cleaning technologies for biomass-derived syngas, *Biomass and Bioenergy.* 52 (2013) 54–84. doi:10.1016/j.biombioe.2013.02.036.
- [18] E. Bocci, A. Di Carlo, S.J. McPhail, K. Gallucci, P.U. Foscolo, M. Moneti, M. Villarini, M. Carlini, Biomass to fuel cells state of the art: A review of the most innovative technology

- solutions, *Int. J. Hydrogen Energy*. 39 (2014) 21876–21895. doi:10.1016/j.ijhydene.2014.09.022.
- [19] R. Di Felice, P. Pagliai, Prediction of the early breakthrough of a diluted H₂S and dry gas mixture when treated by Sulfatreat commercial sorbent, *Biomass and Bioenergy*. 74 (2015) 244–252. doi:10.1016/j.biombioe.2015.01.015.
- [20] E. Pieratti, M. Baratieri, S. Ceschini, L. Tognana, P. Baggio, Syngas suitability for solid oxide fuel cells applications produced via biomass steam gasification process: Experimental and modeling analysis, *J. Power Sources*. 196 (2011) 10038–10049. doi:10.1016/j.jpowsour.2011.07.090.
- [21] L. Barelli, G. Bidini, E. Hernandez-Balada, J. Mata-Avarez, E. Sisani, Performance characterization of a novel Fe-based sorbent for anaerobic gas desulfurization finalized to high temperature fuel cell applications, *Int. J. Hydrogen Energy*. (2016) 1–16. doi:10.1016/j.ijhydene.2016.09.070.
- [22] S. Park, B. Choi, H. Kim, J.-H. Kim, Hydrogen production from dimethyl ether over Cu/ γ -Al₂O₃ catalyst with zeolites and its effects in the lean NO_x trap performance, *Int. J. Hydrogen Energy*. 37 (2012) 4762–4773. doi:10.1016/j.ijhydene.2011.12.038.
- [23] E. Sisani, G. Cinti, G. Discepoli, D. PENCHINI, U. Desideri, F. Marmottini, Adsorptive removal of H₂S in biogas conditions for high temperature fuel cell systems, *Int. J. Hydrogen Energy*. 39 (2014) 21753–21766. doi:10.1016/j.ijhydene.2014.07.173.
- [24] M.D. Ganji, N. Sharifi, M. Ardjmand, M.G. Ahangari, Pt-decorated graphene as superior media for H₂S adsorption: A first-principles study, *Appl. Surf. Sci.* 261 (2012) 697–704. doi:10.1016/J.APSUSC.2012.08.083.
- [25] T.K. Ghosh, E.L. Tollefson, Kinetics and reaction mechanism of hydrogen sulfide oxidation over activated carbon in the temperature range of 125–200°C, *Can. J. Chem. Eng.* 64 (1986) 969–976. doi:10.1002/cjce.5450640613.
- [26] R. Yan, D.T. Liang, L. Tsen, J.H. Tay, Kinetics and Mechanisms of H₂S Adsorption by Alkaline Activated Carbon, *Environ. Sci. Technol.* 36 (2002) 4460–4466. doi:10.1021/es0205840.
- [27] A. Bagreev, S. Katikaneni, S. Parab, T.J. Bandosz, Desulfurization of digester gas: prediction of activated carbon bed performance at low concentrations of hydrogen sulfide, *Catal. Today*. 99 (2005) 329–337. doi:10.1016/j.cattod.2004.10.008.
- [28] A. Bouzaza, A. Laplanche, S. Marsteau, Adsorption-oxidation of hydrogen sulfide on activated carbon fibers: Effect of the composition and the relative humidity of the gas phase, *Chemosphere*. 54 (2004) 481–488. doi:10.1016/j.chemosphere.2003.08.018.
- [29] A. Bagreev, T.J. Bandosz, H₂S adsorption/oxidation on unmodified activated carbons: importance of prehumidification, *Carbon N. Y.* 39 (2001) 2303–2311. doi:10.1016/S0008-6223(01)00049-5.
- [30] I. Isik-Gulsac, Investigation of impregnated activated carbon properties used in hydrogen sulfide fine removal, *Brazilian J. Chem. Eng.* 33 (2016) 1021–1030. doi:10.1590/0104-6632.20160334s20150164.
- [31] H. Wu, Y. Zhu, S. Bian, J.H. Ko, S.F.Y. Li, Q. Xu, H₂S adsorption by municipal solid waste incineration (MSWI) fly ash with heavy metals immobilization, *Chemosphere*. 195 (2018) 40–47. doi:10.1016/j.chemosphere.2017.12.068.
- [32] M. Hervy, D. Pham Minh, C. Gérente, E. Weiss-Hortala, A. Nzihou, A. Villot, L. Le Coq, H₂S removal from syngas using wastes pyrolysis chars, *Chem. Eng. J.* 334 (2018) 2179–2189. doi:10.1016/J.CEJ.2017.11.162.
- [33] F. Marchelli, C. Moliner, M. Curti, G. Rovero, M. Baratieri, B. Bosio, E. Arato, Characterisation of the Char Obtained from Biomass Gasification in a Spouted Bed Reactor, in: *Eur. Biomass Conf. Exhib. Proc.*, 2017: pp. 847–852. doi:10.5071/25thEUBCE2017-2CV.3.47.
- [34] D. Bove, C. Moliner, M. Curti, M. Baratieri, B. Bosio, G. Rovero, E. Arato, Preliminary Tests for the Thermo-Chemical Conversion of Biomass in a Spouted Bed Pilot Plant, *Can. J. Chem. Eng.* (2018). doi:10.1002/cjce.23223.
- [35] P.J.F. Harris, Z. Liu, K. Suenaga, Imaging the atomic structure of activated carbon, *J. Phys. Condens. Matter*. 20 (2008) 362201. doi:10.1088/0953-8984/20/36/362201.
- [36] J.R. Regalbuto, M. Schrier, X. Hao, W.A. Spieker, J.G. Kim, J.T. Miller, A.J. Kropf, Toward a

- molecular understanding of noble metal catalyst impregnation, *Stud. Surf. Sci. Catal.* 143 (2000) 45–53. doi:10.1016/S0167-2991(00)80641-2.
- [37] D. Prando, F. Patuzzi, J. Ahmad, T. Mimmo, M. Baratieri, Environmental Impact of Char from Four Commercial Gasification Systems, *Eur. Biomass Conf. Exhib. Proc.* 2016 (2016) 828–830. doi:10.5071/24thEUBCE2016-2CV.3.9.
- [38] L. Barelli, G. Bidini, N. de Arespacochaga, L. Pérez, E. Sisani, Biogas use in high temperature fuel cells: Enhancement of KOH-KI activated carbon performance toward H₂S removal, *Int. J. Hydrogen Energy.* 42 (2017) 10341–10353. doi:10.1016/j.ijhydene.2017.02.021.
- [39] R. Sitthikhankaew, D. Chadwick, S. Assabumrungrat, N. Laosiripojana, Effect of KI and KOH Impregnations over Activated Carbon on H₂S Adsorption Performance at Low and High Temperatures, *Sep. Sci. Technol.* 49 (2014) 354–366. doi:10.1080/01496395.2013.841240.
- [40] C. HUANG, C. CHEN, S. CHU, Effect of moisture on H₂S adsorption by copper impregnated activated carbon, *J. Hazard. Mater.* 136 (2006) 866–873. doi:10.1016/j.jhazmat.2006.01.025.
- [41] D. Geldart, Types of gas fluidization, *Powder Technol.* 7 (1973) 285–292. doi:10.1016/0032-5910(73)80037-3.
- [42] S. Ergun, Fluid Flow Through Packed Columns, *Chem. Eng. Prog.* 48 (1952) 89–94.